Interaction energy for a pair of quantum wells

Bo E. Sernelius and P. Björk
Department of Physics and Measurement Technology, Linköping University, S-581 83 Linköping, Sweden
(Received 24 February 1997; revised manuscript received 8 September 1997)

We present a calculation of the interaction energy and force between two quantum wells in which the wells are treated as strictly two-dimensional metallic sheets. Numerical results are presented for separation values ranging from 1 to 10^{12} Å. Both nonretarded and retarded calculations are presented. Three distinct ranges with different separation dependences are clearly revealed in the results; the Casimir limit for large separations; the van der Waals range for intermediate separations; the small separation limit where also the single-particle continuum contributes. The result in the Casimir limit coincides with the corresponding result for two metal half-spaces but the van der Waals result is different from both the half-space result and that of two thin films. In the present problem the energy and force varies as $d^{-5/2}$ and $d^{-7/2}$, respectively. [S0163-1829(98)02511-9]

I. INTRODUCTION

In the late 1940s Casimir[1] used a new and very successful approach to calculate the force between neutral objects. He studied two charge-neutral metallic plates. Surprisingly, for large separation this force is independent of the density, charge, and effective mass of the carriers.[2] Instead it depends on the speed of light. He related the force to the change in zero-point electromagnetic energy with distance between the objects. There has been a renewed interest[3,4] in these so-called Casimir forces lately that has inspired the present work. A historical introduction to the field with emphasis on the experimental attempts to verify the Casimir and van der Waals forces is found in the review paper by Elizalde and Romeo.[5] Complimentary reviews can be found where the Casimir effect in other areas, like elementary-particle physics and cosmology, is included.[6] The most detailed and recent verification of the Casimir effect is found in Ref. 7.

Schmit and Lucas[8] and also Craig[9] used a kindred approach to determine the surface energy of simple metals. They attributed this to the change in zero-point energy of the surface plasmons when the metal is split in two and the pieces are separated to infinite distance. Van Kampen, Nijboer, and Schram[10] used the zero-point energy of the surface modes of a dielectric to derive the van der Waals force between two semi-infinite dielectric media. They also demonstrated that the Casimir result was equivalent to that from the macroscopic Lifshitz theory;[11] this theory is rather complicated and involves the introduction of random fluctuating sources inside the dielectrics.

The modes in the two approaches are quite different, but both types of mode are present in the spectral range where the dielectric function of the metal or dielectric has a negative value. In the Casimir case they are formed from purely transverse, freely propagating electromagnetic waves (photons) multiple-reflected at the surfaces of the two metals or dielectrics; the net result is modes of standing-wave- or wave-guide-type. In the van der Waals case they are modes that are localized to the surfaces of the objects (exponentially decaying outside the objects). Both types of mode are present and contribute to the energy of the system and the force between the objects, but they dominate the force in different separation ranges. For both types of mode the fields decay exponentially inside the material. The induced charges and currents are localized to the surfaces. In the van der Waals case, when the force between two metal or dielectric plates is considered, there are two modes; one with higher energy and one with lower, both of p-polarized type; for the high- (low-) energy mode the induced charge and current are even (odd) with respect to a plane in the middle between the surfaces; the energy of these modes changes with separation, and this change causes the force. In the Casimir case there are many standing-wave-type modes of both p-polarized (TE modes) and s-polarized (TM modes) type; the number of modes and their energies change with separation, and these changes cause the force.

In the present work, we study a model system of two strictly two-dimensional (2D) metallic sheets. Since it does not add to the complexity we have let the sheets be embedded in a dielectric medium. This model system very well represents the ''current-drag'' system of Ref. 12. This system consists of two narrow electron quantum wells in GaAs. Each well can to a good approximation be treated as strictly 2D as long as the following two conditions are fulfilled: the separation between the wells is big enough, so that the wave functions in the different wells are not overlapping; the wells are narrow enough so that in each well only one level is occupied and the closest unoccupied level is far enough up in energy for interband transitions to be negligible.

We study how the interaction energy and the attractive force between these sheets vary with separation. We make both nonretarded and retarded calculations. We first perform the nonretarded calculations, which are simpler. The interaction energy is just the correlation energy between the sheets. In Sec. II we very briefly describe the system and its dielectric properties. The dielectric properties of 2D, quasi-2D, and coupled 2D systems and their collective modes have been studied extensively in the past[13–19] so we keep the presentation of these properties to a minimum. In Sec. III we present the calculation of the correlation energy and in Sec. IV we perform a calculation based on the zero-point energy of the plasmon modes. In the full retarded calculation both longitudinal and transverse interactions contribute. These calculations are presented in Sec. V. Section VI is devoted to the

 © 1998 The American Physical Society

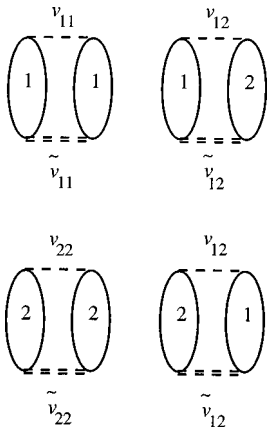

FIG. 1. Feynman diagrams for the correlation energy in our two-layer system. The ellipses represent polarization bubbles and the dashed lines the interactions indicated in the figure. The numbers 1 and 2 refer to which well the electron belongs to.

presentation of the numerical results and comparison between the different approaches. The asymptotic Casimir and van der Waals limits are also given. Finally, Sec. VII contains summary and conclusions.

II. THE SYSTEM

We have chosen to perform our calculations on the ''current-drag'' system of Ref. 12. This system consists of two narrow electron quantum wells in GaAs. The electron density ρ_0 is in each well 1.5×10^{11} cm^{-2}. The effective mass m^* in the conduction band of GaAs is 0.0665 electron masses and we use the value 13.0 for the background dielectric constant κ. We have treated each well as strictly 2D. We have further limited ourselves to $T=0$. In an interacting electron system the energy consists of kinetic energy, exchange energy, and correlation energy. The correlation energy is, per definition, the additional energy contribution beyond the Hartree-Fock approximation. Since there is no overlap between wave functions in neighboring wells there is no interwell exchange energy and the kinetic energy and ordinary intrawell exchange energy are independent of separation. Thus the only energy that changes with separation is the correlation energy.

For the calculations we need the dielectric properties of the system. The elements of the dielectric matrix when retardation effects are neglected are easily found: For inlayer screening,

$$\varepsilon_{22}^{-1}=\varepsilon_{11}^{-1}=\frac{V_1}{V_{\rm ext}^{(1)}}=\frac{1+\alpha_0(1-c_q^2)}{1+2\alpha_0+\alpha_0^2(1-c_q^2)}$$
$$=\frac{1+\alpha_0(1-c_q^2)}{[1+\alpha_0(1+c_q)][1+\alpha_0(1-c_q)]};$$

for interlayer screening,

$$\varepsilon_{21}^{-1}=\varepsilon_{12}^{-1}=\frac{V_2}{V_{\rm ext}^{(2)}}=\frac{1}{1+2\alpha_0+\alpha_0^2(1-c_q^2)}$$
$$=\frac{1}{[1+\alpha_0(1+c_q)][1+\alpha_0(1-c_q)]},$$

where $c_q=\exp(-qd)$ and $\alpha_0(q,\omega)$ is the 2D polarizability.[13,14] The potentials $V_{\rm ext}^{(1)}$, $V_{\rm ext}^{(2)}$, V_1, and V_2 are the external potential from an external charge distribution placed in layer 1, the corresponding potential in layer 2, the resulting potential in layer 1 when the potentials from all induced charges are taken into account, and the resulting potential in layer 2, respectively.

III. CORRELATION ENERGY APPROACH

In this section we make a strict nonretarded derivation of the interaction energy between two quantum wells. As we mentioned in the previous section, for separations large enough so that there is no overlap between the wave functions in different wells the only energy contribution that depends on separation is the correlation energy. The exchange and kinetic energies are constant.

The correlation energy per electron in a 3D or 2D system is in the RPA (random-phase approximation) given by[20]

$$E_c^{\rm RPA}=-\frac{1}{2N}{\sum_{\mathbf{q}}}'\times\left\{\int_{-\infty}^{\infty}\frac{d\omega}{2\pi}\hbar\int_0^1 d\lambda\left[\frac{-\alpha_0'(\mathbf{q},\omega)}{1+\lambda\alpha_0'(\mathbf{q},\omega)}+\alpha_0'(\mathbf{q},\omega)\right]\right\}$$
$$=-\frac{1}{2N}{\sum_{\mathbf{q}}}'\times\left\{\int_{-\infty}^{\infty}\frac{d\omega}{2\pi}\hbar[-\ln[1+\lambda\alpha_0'(\mathbf{q},\omega)]+\lambda\alpha_0'(\mathbf{q},\omega)]_0^1\right\}$$
$$=-\frac{1}{2N}{\sum_{\mathbf{q}}}'\times\left\{\int_{-\infty}^{\infty}\frac{d\omega}{2\pi}\hbar\{\alpha_0'(\mathbf{q},\omega)-\ln[1+\alpha_0'(\mathbf{q},\omega)]\}\right\},$$

where N is the total number of electrons and $\alpha_0'(\mathbf{q},\omega)=\alpha_0(\mathbf{q},i\omega)$, i.e., the polarizability calculated on the imaginary frequency axis.[21] The prime on the summation symbol denotes that the $\mathbf{q}=\mathbf{0}$ term is excluded from the summation. In two dimensions the polarizability is expressed in our dimensionless variables:

$$Q=\frac{q}{2k_0},\quad k_0=(2\pi\rho_0)^{1/2},$$

$$W=\frac{\hbar\omega}{4E_0},\quad E_0=\frac{\hbar^2k_0^2}{2m^*},$$

$$y=\frac{m^*e^2}{\hbar^2\kappa k_0},$$

where k_0 is the Fermi wave number, as

$$\alpha_0'(Q,W)=\alpha_0(Q,iW)$$
$$=y\,\frac{1}{Q}\left\{1-\frac{1}{Q^2}\left[\tfrac{1}{2}\sqrt{(Q^4-W^2-Q^2)^2+(2WQ^2)^2}\right.\right.$$
$$\left.\left.+\tfrac{1}{2}(Q^4-W^2-Q^2)\right]^{1/2}\right\}.$$

The correlation energy per electron in two dimensions is given as

$$E_c^{\mathrm{RPA}}=-\frac{\hbar}{4\pi^2\rho_0}\int_0^\infty\int_0^\infty d\omega\;dq\;q\{\alpha_0'(q,\omega)$$
$$-\ln[1+\alpha_0'(q,\omega)]\}.$$

In the present system with two metallic sheets a distance d apart we get the Feynman diagrams in Fig. 1. These diagrams represent the energy

$$E_c^{\mathrm{RPA}}=-\frac{1}{2N}{\sum_{\mathbf{q}}}'\left\{\int_{-\infty}^{\infty}\frac{d\omega}{2\pi}\,\hbar\int_0^1 d\lambda\{\lambda[\alpha_0'(\mathbf{q},\omega)]^2\varepsilon_{11}^{-1}(\mathbf{q},i\omega)\right.$$
$$\left.+\lambda[\alpha_0'(\mathbf{q},\omega)]^2\varepsilon_{22}^{-1}(\mathbf{q},i\omega)+2\lambda[c_q\alpha_0'(\mathbf{q},\omega)]^2\varepsilon_{12}^{-1}(\mathbf{q},i\omega)\}\right\}$$
$$=-\frac{1}{2N}{\sum_{\mathbf{q}}}'\int_{-\infty}^{\infty}\frac{d\omega}{2\pi}\,\hbar\int_0^1 d\lambda\,\frac{2\lambda\alpha_0'^2}{1+2\lambda\alpha_0'+\lambda^2\alpha_0'^2(1-c_q^2)}\,[1+\lambda\alpha_0'(1-c_q^2)+c_q^2]$$
$$=-\frac{1}{2N}{\sum_{\mathbf{q}}}'\int_{-\infty}^{\infty}\frac{d\omega}{2\pi}\,\hbar\int_0^1 d\lambda\left[2\alpha_0'-\frac{2\alpha_0'+2\lambda\alpha_0'^2(1-c_q^2)}{1+2\lambda\alpha_0'+\lambda^2\alpha_0'^2(1-c_q^2)}\right]$$
$$=-\frac{\hbar}{N}{\sum_{\mathbf{q}}}'\int_{-\infty}^{\infty}\frac{d\omega}{2\pi}\,(\alpha_0'(\mathbf{q},\omega)-\tfrac{1}{2}\ln\{1+2\alpha_0'(\mathbf{q},\omega)+[\alpha_0'(\mathbf{q},\omega)]^2(1-c_q^2)\}),$$

where N is the total number of electrons in the two wells taken together. Thus we have

$$E_c^{\mathrm{RPA}}=-\frac{\hbar}{4\pi^2\rho_0}\int_0^\infty\int_0^\infty d\omega\;dq\;q\{\alpha_0'(q,\omega)$$
$$-\tfrac{1}{2}\ln[1+2\alpha_0'(q,\omega)+\alpha_0'^2(q,\omega)(1-c_q^2)]\}.$$

With the energy at infinite separation as reference energy the above result can be reduced to

$$E_c^{\mathrm{RPA}}(d)-E_c^{\mathrm{RPA}}(\infty)=\frac{\hbar}{4\pi^2}\int_0^\infty\int_0^\infty d\omega\;dq\;q$$
$$\times\ln\left[1-\frac{c_q^2\alpha_0'^2(q,\omega)}{[1+\alpha_0'(q,\omega)]^2}\right],$$

where we have multiplied with $2\rho_0$ to get the total correlation energy per unit area. This is the final result. It is represented by curve 1 in Fig. 3 of Sec. VI.

IV. INTERACTION ENERGY AS CHANGE IN ZERO-POINT PLASMON-ENERGY

The dispersions of the collective modes of our system are obtained as the $\omega(q)$ for which the inverse dielectric functions of Sec. II diverge (or, equivalently, when the determinant of the dielectric matrix is zero). For this choice of ω and q we may have an induced electric field even in the absence of external perturbations. Thus, the dispersion curves for the collective modes are obtained as solutions when the denominator (the interlayer and intralayer versions of the inverse dielectric function have the same denominator) is put equal to zero. At infinite separation the denominator is just the 2D dielectric function squared. This function is zero on the plasmon dispersion curve. Thus we have two degenerate solutions in this limit. When the separation decreases the degeneracy is lifted. One curve moves upwards and the other downwards. This is illustrated in Fig. 2 which is valid for

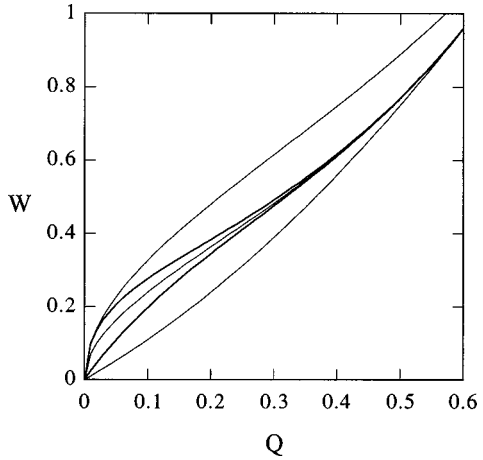

FIG. 2. The dispersion of the collective modes. The thick curves are the dispersions of the two modes for the well separation 500 Å. The uppermost thin curve is the asymptotic limit for the upper mode at zero separation. The thin curve in the middle is the asymptotic limit for both modes at infinite separation. The lower thin curve is the upper boundary of the single-particle continuum.

$d=500$ Å. At zero separation the lower one is pushed completely into the continuum and the upper one is the solution to the equation $1+2\alpha_0(q,\omega)=0$.

All the modes, for increasing q, sooner or later enter the continuum. The number of modes does not decrease with one each time a mode enters the continuum. The number of continuum modes increases with one at this point. We are facing a problem with this approach since we cannot determine where each mode goes. The energy of the collective mode is shared among the continuum modes. This problem was avoided by Schmit and Lucas and Craig by using their drastic approximations. We use the approximation that the mode stays at the boundary of the continuum. With this approximation we get for the energy

$$E(d)=\sum_{\mathbf{q}}\left\{\left[\frac{\hbar}{2}\,\omega_1(q,d)+\frac{\hbar}{2}\,\omega_2(q,d)\right]-\left[\frac{\hbar}{2}\,\omega_1(q,\infty)+\frac{\hbar}{2}\,\omega_2(q,\infty)\right]\right\}$$
$$=A\int_0^\infty\frac{d^2q}{(2\pi)^2}\left\{\left[\frac{\hbar}{2}\,\omega_1(q,d)+\frac{\hbar}{2}\,\omega_2(q,d)\right]-\left[\frac{\hbar}{2}\,\omega_1(q,\infty)+\frac{\hbar}{2}\,\omega_2(q,\infty)\right]\right\},$$

where $\omega_1(q,d)$ and $\omega_2(q,d)$ are the two collective modes and A is the area of each quantum well. We have used the energy at infinite separation as our reference energy. The result from this calculation is represented by curve 2 in Fig. 3 of Sec. VI.

V. RETARDATION EFFECTS

We have chosen to work in Coulomb gauge. In this gauge one part of the interaction between the electrons is in the form of the instantaneous, longitudinal Coulomb interaction (scalar potential) and the other part is via transverse photons (vector potential.) The Hamiltonian for the system is

$$H=\sum_i\frac{1}{2m^*}\left[\mathbf{p}_i-\frac{e_i}{c}\,\mathbf{A}(\mathbf{r}_i)\right]^2+\frac{1}{2}\sum_{ij}\frac{e_ie_j}{\kappa r_{ij}}+\sum_{\mathbf{k},\lambda}\hbar\omega_{\mathbf{k}}(a^\dagger_{\mathbf{k}\lambda}a_{\mathbf{k}\lambda}+\tfrac{1}{2}),$$

where the first term is the kinetic energy that contains the interactions via the vector potential **A**. The second term represents the scalar potential interaction and the last term is the free photon Hamiltonian. For very large separations between the wells we need to take retardation effects into account. If the distance between two electrons is smaller than $\tilde{c}/\omega$, retardation effects in the interaction between the electrons can be neglected. We let $\tilde{c}$ denote the speed of light in the medium surrounding the wells. The nonretarded results are obtained by letting the speed of light tend to infinity. From the Hamiltonian we see that this corresponds to neglecting the vector-potential interaction completely. Now, in the specific system we consider here, the electrons are only free to move in a plane. In a plane only one longitudinal and one transverse electric field can exist. It turns out that the longitudinal electric field and the p-polarized photons combine into one field that is longitudinal in the plane. The induced charge and current densities from such a field will also produce a field of that kind. The s-polarized photons produce an electric field that is transverse in the plane. The current induced by such a field produces a field of the same type. In a translational invariant and homogeneous system there are three types of normal modes; two with transverse fields and one with longitudinal fields. In the present system there are only two types of normal modes; one with p-polarized fields, i.e., with electric vector in the plane formed by the in-plane momentum **q** and the normal to the wells, experienced as longitudinal in the 2D sheets; one with s-polarized fields, i.e., with electric vector perpendicular to this plane, experienced as transverse in the 2D sheets.

The two types of interaction involving longitudinal and transverse electric fields in the planes defined by the two sheets will not mix and the energy is given by a sum of two sets of diagrams of the type given in Fig. 1, one set for the longitudinal interaction and one containing only transverse interactions. Let us now discuss the longitudinal interaction. The coupling to the longitudinal field and p-polarized photons is given by the scalar potential and the $\mathbf{p}\cdot\mathbf{A}$ terms in the Hamiltonian. The resulting interaction energy per unit area is

$$E_{l+p}(d)=\frac{\hbar}{4\pi^2}\int_0^\infty\int_0^\infty d\omega\;dq\;q\;\ln\left\{1-e^{-2qd\gamma'(q,\omega)}\times\left[\frac{\gamma'(q,\omega)\alpha_0'(q,\omega)}{1+\gamma'(q,\omega)\alpha_0'(q,\omega)}\right]^2\right\}.$$

This energy is represented by curve 4 in Fig. 3 of Sec. VI. The derivation of this expression is given in the Appendix. Compared with the nonretarded result for the correlation energy, we gave earlier, we find that the polarizability has attained a factor $\gamma'(q,\omega)=\gamma(q,i\omega)=\sqrt{1+(\omega/\tilde{c}q)^2}$ in front, which is in agreement with the polarizability obtained by Stern.[14] Furthermore, the factor appearing in the interwell interactions is modified according to $c_q\rightarrow c_{q,i\omega}=e^{-qd\gamma'(q,\omega)}$.

The response to the s-polarized fields is a transverse current. It is described by the transverse conductivity, which is completely dominated by the contribution originating from the A^2 term in the Hamiltonian. Also the $\mathbf{p}\cdot\mathbf{A}$ terms in the Hamiltonian give a contribution to the transverse conductivity, in the form of the current-current correlation function. We have derived this function for two dimensions. It has negligible effects for the present problem but we still give the function in the Appendix.

The energy per unit area from the s-photon interaction is

$$E_s(d)=\frac{\hbar}{4\pi^2}\int_0^\infty\int_0^\infty d\omega\;dq\;q\;\ln\left\{1-e^{-2qd\gamma'(q,\omega)}\times\left[\frac{2\pi e^2\rho_0/qm^*c^2\gamma'(q,\omega)}{1+2\pi e^2\rho_0/qm^*c^2\gamma'(q,\omega)}\right]^2\right\}.$$

The result is represented by curve 3 in Fig. 3 of Sec. VI. The derivation of this expression is given in the Appendix.

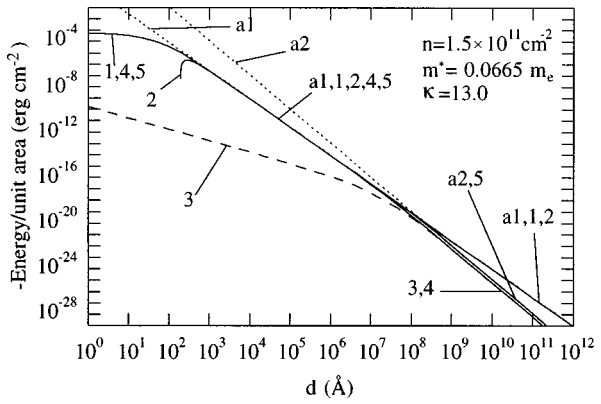

FIG. 3. The interaction energy per unit area for our model system as function of separation, with parameters in accordance with the ''current drag'' system of Ref. 12. The dotted lines $a1$ and $a2$ are the large separation asymptotes for the van der Waals and Casimir energies, respectively. Curves 1 and 2 are the nonretarded results from the correlation-energy and plasmon zero-point-energy approaches, respectively. Curves 3 and 4 are the retarded contributions from the s-polarized and longitudinal plus p-polarized interactions, respectively. The total retarded result, i.e., the sum of curves 3 and 4, is represented by curve 5.

VI. NUMERICAL RESULTS

The main result of this work is presented in Fig. 3. We present all results in the form of the interaction energy E per unit area. The force F is obtained from these results just by performing the derivative with respect to separation. The asymptotes $a1$ and $a2$ represent the van der Waals and Casimir results, respectively. They are the large separation limits of the nonretarded and retarded treatments, respectively. The van der Waals result, $a1$, depends on the material parameters according to

$$E \approx -0.012\,562 e\hbar \sqrt{\rho_0/\kappa m^*} d^{-5/2},$$

$$F \approx 0.031\,406 e\hbar \sqrt{\rho_0/\kappa m^*} d^{-7/2}.$$

This d dependence is different from the behavior of two semi-infinite solids[10,22,23] where E and F depend on d as d^{-2} and d^{-3}, respectively. It does not agree with the result for two thin films either where the dependences are d^{-4} and d^{-5}, respectively.[22,23]

The Casimir result, $a2$, on the other hand, agrees with the result for two semi-infinite metals. It is

$$E = -\frac{\hbar \tilde{c} \pi^2}{720 d^3},$$

$$F = \frac{\hbar \tilde{c} \pi^2}{240 d^4}.$$

The asymptote $a2$ has a steeper slope than $a1$ and the two asymptotes cross at the separation $d \approx 1.1907 m^* c^2/\rho_0 e^2$. It is to be noted that $a2$ does not depend on the material parameters of the sheets. The reason is the following.

In our expression for the retarded contribution from the longitudinal and p-polarized interaction the exponential factor in the integrand guarantees that the region near the origin only of the ωq plane contributes. There, $\alpha_0'(q,\omega)$ is very large, which means that the polarizabilities in the numerator and denominator cancel out. We get the following contribution:

$$E(d)_{\text{long}} \approx \frac{\hbar}{4\pi^2} \int_0^\infty \int_0^\infty d\omega\, dq\, q\, \ln[1 - e^{-qd\sqrt{1+(\omega/\tilde{c}q)^2}}]$$

$$= -\frac{\hbar \tilde{c} \pi^2}{480 \times 3 d^3}.$$

The same applies for the contribution that comes from the s-polarized interaction and it gives an identical result. The polarizabilities and hence all material parameters completely drop out of the expressions for large distances.

Curve 1 represents our full nonretarded result from the correlation-energy calculation. It approaches the van der Waals result for intermediate and large separation. In the correlation energy both single-particle and collective excitations contribute. The result is obtained as an integral over the ωq plane. In the small-q limit the contributions from the collective excitations dominate, and one can show that these contributions are just the zero-point energy of the modes. The exponential factor in the integrand guarantees that for large separations only the small momentum region contributes. Hence, in that limit the correlation energy approaches the zero-point energy of the modes.

Curve 2 is the result from the calculation where the interaction energy comes entirely from the zero-point energy of the plasmon modes. We find that with this approach we actually get a repulsive force for small separations and a negative adhesion energy. As we mentioned earlier we let the modes stay at the boundary of the continuum instead of entering it. Another possibility would be to let the modes drop to zero energy as soon as they enter the continuum. We have also calculated the energy and force with this approximation. The results are quantitatively quite different but qualitatively the same, with a repulsive force at short range. For intermediate and large separations the result merges with curve 1 and the van der Waals result, $a1$, and the result is independent of how we treat the modes when they merge with the single-particle continuum. Thus for large separations the approach where only the zero-point energy of the plasmons is calculated works well and since this means a simpler calculation this approach may be preferable. This is no longer true for very large separations where the retardation effects become dominant. It turns out that in this regime the force caused by the Coulomb interaction is suppressed and replaced by photon interactions. In the correlation energy approach both the longitudinal collective excitations and transverse single-particle excitations contribute to the energy. For large separations and neglect of retardation effects the collective part dominates the force. When retardation effects are included the collective part of the force is suppressed and another contribution appears. This contribution turns up as an imaginary part in $\gamma\alpha_0$ for frequencies above the dispersion curve for the light. It has its origin in emission of the

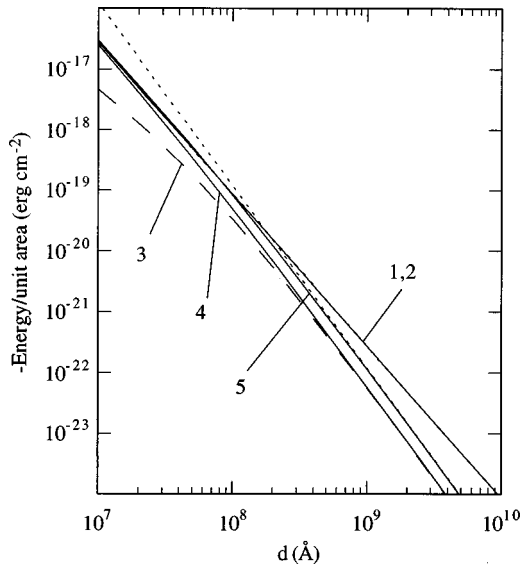

FIG. 4. An expanded view of the bifurcation region of Fig. 3.

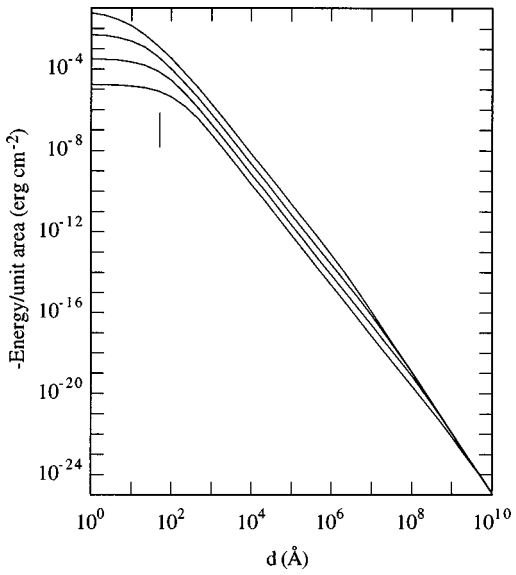

FIG. 5. Our full retarded results for the interaction energy per unit area as functions of separation for the carrier densities 1×10^{10}, 1×10^{11}, 1×10^{12}, and 1×10^{13} cm^{-2}, respectively. The magnitude of the energy increases with density. The vertical bar indicates the point where the separation equals the two-dimensional Thomas-Fermi screening length.

transverse photons. That this is so is especially obvious in the case of s-polarized photons, where there are no collective plasmon modes at all, but we still get the same contribution to the force as from the p-polarized ones. Curve 3 is the contribution from s-polarized photons. Curve 4 represents the contribution from the longitudinal and p-polarized interactions. It reproduces the full nonretarded result for small and intermediate separations. When it approaches asymptote $a2$ it changes direction and follows a curve representing half of the Casimir result. The total retarded result, i.e., the sum of curves 3 and 4, is represented by curve 5. This full result coincides with the nonretarded result for small and intermediate separations and with the Casimir result for large separations. For large separations the scalar-potential contribution is suppressed and partly canceled by the vector-potential contribution. This is maybe most clearly seen in the dispersion curves of the plasmon modes. These are, when retardation is taken into account, in the long-wavelength limit pushed down below the dispersion curve for the light.

One interesting thing to notice is that the full result does not follow the upper one of the two asymptotes $a1$ and $a2$. Instead, it follows the lower one. This is contrary to what one would imagine since the result is the sum of the plasmon and photon contributions. The reason is that when the photons start to contribute the plasmon contribution drops in size, and vice versa.

The full nonretarded and full retarded results are the same for small and intermediate separations but split up for larger separations. In Fig. 4 we have expanded the bifurcation region. Figure 5 shows the full retarded results for different carrier concentrations. The curves are shifted towards higher energies with increasing densities but they all approach the same density-independent asymptote for large separations. In the figure we have given the results for the densities 1×10^{10}, 1×10^{11}, 1×10^{12}, and 1×10^{13} cm^{-2}, respectively. These examples span the reasonable density range for the real system we have chosen to model. The vertical bar in the figure indicates the 2D Thomas-Fermi screening length which is density independent, in contrast to the case in three dimensions. There is a clear connection between this screening length and the separation where the short-range, single-particle correlations become important.

It is of experimental interest to find an estimate of the maximum possible Casimir force in our system. If we make the approximation that the van der Waals and Casimir forces represent the actual force to the left and right of, respectively, and all the way up to the crossing point between asymptotes $a1$ and $a2$, we find that the maximum Casimir force is $F_{\max}^{\text{Casimir}}\approx 0.02\rho_0^4\hbar e^8/\sqrt{\kappa}(m^*)^4c^7$. The result depends strongly on both the carrier density and the effective mass. One should choose as high a density and as small an effective mass as possible if the goal is to study the Casimir force experimentally.

VII. SUMMARY AND CONCLUSIONS

We have determined the energy and force as functions of separation between two two-dimensional metallic sheets—a model system representing a pair of quantum wells. We performed both nonretarded and retarded calculations.

The nonretarded calculations were performed with two different approaches. In one approach the energy variation with separation was attributed to the change in zero-point energy of the collective modes of the system. We found that the result for small separations was sensitive to the unavoidable approximations concerning how to treat the modes when they enter the single-particle continuum. The approach led to a force that is attractive at long range but repulsive at short range. With the approximations we used, the adhesion energy was negative. In the other, more strict, approach we calculated the correlation energy in the random-phase approximation. This led to an attractive force at all distances. The forces in the two nonretarded approaches merge for large separation and have the asymptotic form $\sim d^{-7/2}$. These forces drop off faster than that derived from semi-

infinite metallic plates and more slowly than in the case of two thin films. The forces depend on the electron density and electron effective mass. Improvements of the theory by going beyond RPA through the inclusion of local-field corrections would be much more complicated,[25,26] only modify the results for small separations and would not change the asymptotic form of the forces. For small separations there would, in a real system, be other complications from short-range forces on the atomic scale, effects from imperfections like interface roughness and sooner or later, when the distance between the wells decreases further, effects from carrier tunneling between the wells and interlayer exchange effects. All these effects are beyond the scope of the present work.

The cause of the differences in asymptotic form for the present system and the thick-metal-plate case is the difference in dispersion of the collective modes: In the present case the dispersion is of square-root type while the dispersion of the surface plasmon in the thick-metal-plate case starts out as constant for small momenta. In the thin-metal-film case the modes on the back sides of the films interfere and contribute; thus there are four modes contributing to the interaction and hence the different asymptotic behavior is not surprising.

In the full retarded calculation both longitudinal and transverse interactions contribute. The result coincides with the full nonretarded result for small and intermediate separations but drastically changes character when the Casimir asymptote is approached; then it follows this asymptote and becomes independent of the material parameters of the sheets. That the results in this limit agree with those of the thick-metal-plate case is not too surprising. In this limit the fields are totally reflected and these boundary conditions are the same in both cases. The material parameters are only important at which separation the Casimir limit is reached.

The maximum force obtained for our model system is not very large, around 10^6 dyn/cm^{-2} (10^5 N/m^{-2}) for the wells with highest electron concentration. Expressed in another way, it is roughly one-tenth of the electrostatic repulsive force between the electrons in the two wells. The effects from these forces on the system are probably small. One way to measure the forces between quantum wells would be to use an atomic force microscope and let one of the wells be in the tip and the other below, but very close to the surface.

In summary, different contributions to the force dominate for different separations. For small separations, of the order of the Thomas-Fermi screening length and smaller, both single-particle and collective longitudinal excitations contribute; in the intermediate separation range collective longitudinal excitations completely dominate; for large separations the contributions from collective longitudinal excitations are suppressed and replaced by contributions from collective transverse excitations. Our numerical results are valid for all separations and clearly demonstrate the crossover between the three interaction regimes.

ACKNOWLEDGMENT

We gratefully acknowledge financial support from the Swedish Natural Science Research Council.

APPENDIX

In this appendix we derive the longitudinal and transverse polarizabilities $\tilde{\alpha}_0^{\,l}$ and $\tilde{\alpha}_0^{\,t}$, respectively, when retardation is taken into account. To find these we study the response of a single layer at $z=0$ to an applied electric field, longitudinal or transverse. The induced currents and charge densities in the layer lead to an induced field in and outside the layer. The polarizabilities are identified through the relation between the induced and the total fields in the layer. If we instead use the induced field in a layer at $|z|=d$ we may also identify the factor $c_{q,\omega}$, replacing c_q, which appeared in the nonretarded case. We have

$$E_{\rm ind}^{l,t}(q,z;\omega)=-\tilde{\alpha}_0^{\,l,t}(q;\omega)c_{q,\omega}(z)E_{\rm tot}^{l,t}(q,z=0;\omega),$$

where the superscripts l or t indicate if the fields are longitudinal or transverse, respectively. The fields are the components of the fields in the plane of the layers and longitudinal and transverse here mean the field components that are parallel and perpendicular (but still in the plane) to the momentum $\mathbf{q}$.

Longitudinal polarizability

Let us first start with the longitudinal case. We choose to let the momentum point in the x direction. We apply an external longitudinal electric field, which then also points in the x direction. Thus we have

$$E_{\rm ext}(x,y,0;t)=E_{\rm ext}(q,0,0;\omega)e^{i(qx-\omega t)}.$$

This field will lead to both an induced charge density and an induced current density. These are not independent but related through the continuity equation. The charge density is

$$\rho(x,-,z,t)=\rho(q,0,-;\omega)e^{i(qx-\omega t)}\delta(z)$$
$$=\frac{1}{L}\sum_{q_z}\rho(q,0,-;\omega)e^{i(q_x x+q_z z-\omega t)}.$$

This charge density is independent of the y coordinate and its Fourier transform is independent of q_z. The current density must point inside the layer. Hence, the z component must be 0. Use of the continuity equation,

$$\frac{\partial\rho(\mathbf{r},t)}{\partial t}=-\nabla\cdot\mathbf{j}(\mathbf{r},t),$$

leads to

$$-i\mathbf{q}\cdot\mathbf{j}(q,0,q_z;\omega)=-i\omega\rho(q,0,-;\omega),$$

which means that the current must point in the x direction. We have

$$j(q,0,-;\omega)=\frac{\omega}{q}\rho(q,0,-;\omega).$$

Now, we are interested in the induced electric field. The electric field depends on both the scalar and vector potentials, according to

$$\mathbf{E}=-\nabla\varphi-\frac{1}{c}\frac{\partial}{\partial t}\mathbf{A}.$$

We use Coulomb guage where the scalar potential is instantaneous and the vector potential transverse. In Coulomb gauge we have

$$\nabla^2\varphi=-\frac{4\pi\rho}{\kappa},$$

$$\nabla^2\mathbf{A}-\frac{\kappa}{c^2}\frac{\partial^2}{\partial t^2}\mathbf{A}=-\frac{4\pi}{c}\mathbf{j}_t,$$

which means that

$$\varphi=\frac{4\pi\rho}{\kappa\tilde{q}^{\,2}},$$

$$\mathbf{A}=\frac{4\pi}{c\left[\tilde{q}^{\,2}-\kappa\left(\frac{\omega}{c}\right)^2\right]}\mathbf{j}_t.$$

The $\tilde{\mathbf{q}}$ in these last relations is a general $\tilde{\mathbf{q}}$ that need not point inside the layer and the index t means the transverse part of the current density, i.e., the component along this $\tilde{\mathbf{q}}$ is subtracted from the total current density. The induced field is

$$\mathbf{E}_{\rm ind}(q,0,q_z;\omega)=i(\mathbf{q}_x+\mathbf{q}_z)\frac{-4\pi}{\kappa\tilde{q}^{\,2}}\rho(q,0,-;\omega)+i\omega\frac{4\pi}{c^2\left[\tilde{q}^{\,2}-\kappa\left(\frac{\omega}{c}\right)^2\right]}\mathbf{j}_t(q,0,q_z;\omega).$$

The first term is a longitudinal field and the second a p-polarized transverse one. In the plane itself they are indistinguishable. They are both experienced as longitudinal. Now, we have

$$\mathbf{E}_{\rm ind}(q,0,q_z;\omega)=i(\mathbf{q}_x+\mathbf{q}_z)\frac{-4\pi}{\kappa\tilde{q}^2}\rho(q,0,-;\omega)+i\omega\frac{4\pi}{c^2\left[\tilde{q}^{\,2}-\kappa\left(\frac{\omega}{c}\right)^2\right]}\frac{q_z}{\tilde{q}}\times\left(\frac{q_z}{\tilde{q}}\hat{x}-\frac{q}{\tilde{q}}\hat{z}\right)\frac{\omega}{q}\rho(q,0,-;\omega).$$

As can be seen there is, apart from the field in the x direction, which is the field we are interested in, also a field in the z direction. The carriers can only respond to the field in the x direction. This field is

$$E_{\rm ind}(q,0,q_z;\omega)=iq\frac{-4\pi}{\kappa\tilde{q}^{\,2}}\rho(q,0,-;\omega)\times\left[1+\frac{\kappa\left(\frac{\omega}{c}\right)^2}{\left[\kappa\left(\frac{\omega}{c}\right)^2-\tilde{q}^{\,2}\right]}\frac{q_z^2}{q^2}\right]=-i\frac{4\pi}{\kappa q^2}\rho(q,0,-;\omega)\left[\frac{\kappa\left(\frac{\omega}{c}\right)^2-q^2}{\kappa\left(\frac{\omega}{c}\right)^2-\tilde{q}^{\,2}}\right].$$

We want the z dependence of the induced field, which is obtained by taking the inverse Fourier transform of this expression with respect to q_z. The result is

$$\begin{aligned}E_{\rm ind}(q,0,z;\omega)&=-i\frac{2\pi}{\kappa q^2}\rho(q,0,-;\omega)\times\left[\frac{q^2-\kappa\left(\frac{\omega}{c}\right)^2}{\sqrt{q^2-\kappa(\omega/c)^2}}\right]e^{-\sqrt{q^2-\kappa(\omega/c)^2}|z|}\\&=-i\frac{2\pi}{\kappa q}\rho(q,0,-;\omega)\times\sqrt{1-\kappa(\omega/qc)^2}e^{-\sqrt{1-\kappa(\omega/qc)^2}q|z|}\\&=-i\frac{2\pi}{\kappa q}\rho(q,0,-;\omega)\gamma(q,\omega)e^{-\gamma(q,\omega)q|z|}\\&=-\alpha_0(q;\omega)E_{\rm tot}(q,z=0;\omega)\times\gamma(q,\omega)e^{-\gamma(q,\omega)q|z|},\end{aligned}$$

where

$$\gamma(q,\omega)=\sqrt{1-\kappa(\omega/qc)^2}=\sqrt{1-(\omega/q\tilde{c})^2}.$$

In the plane we have

$$\begin{aligned}E_{\rm ind}(q,0,z=0;\omega)&=-\alpha_0(q;\omega)\gamma(q,\omega)E_{\rm tot}(q,z=0;\omega)\\&=-\tilde{\alpha}^{\,l}_0(q;\omega)E_{\rm tot}(q,z=0;\omega).\end{aligned}$$

In the other plane we have

$$\begin{aligned}E_{\rm ind}(q,0,|z|=d;\omega)&=-\alpha_0(q;\omega)\gamma(q,\omega)e^{-\gamma(q,\omega)qd}\times E_{\rm tot}(q,z=0;\omega)\\&=-\tilde{\alpha}^{l}_0(q;\omega)c_{q,\omega}E^{l}_{\rm tot}(q,z=0;\omega).\end{aligned}$$

From these relations we find that the longitudinal interaction is the same as without retardation except for the following changes:

$$\alpha_0(q;\omega)\rightarrow\tilde{\alpha}^{\,l}_0(q;\omega)=\gamma(q,\omega)\alpha_0(q;\omega),$$

$$c_q\rightarrow c_{q,\omega}=e^{-\gamma(q,\omega)qd}.$$

Transverse polarizability

Let us now treat the transverse case. We still choose to let the momentum point in the x direction. We apply an external transverse electric field, which then points in the y direction. Thus we have

$$E_{\rm ext}(x,y,0;t)=E_{\rm ext}(q,0,0;\omega)e^{i(qx-\omega t)}.$$

The net induced current density is

$$\begin{aligned}\mathbf{j}_y(\mathbf{r},t)&=\mathbf{j}_y(q,0,-;\omega)e^{i(qx-\omega t)}\delta(z)\\&=\frac{1}{L}\sum_{q_z}\mathbf{j}_y(q,0,-;\omega)e^{i(qx+q_zz-\omega t)}.\end{aligned}$$

The current density is pointing in the y direction and is independent of the y coordinate and its Fourier transform is independent of q_z. This current contributes to the vector potential, which in turn contributes to the induced electric field:

$$\begin{aligned}\mathbf{E}_{\rm ind}(q,0,q_z;\omega)&=i\,\frac{\omega}{c}\,\mathbf{A}(q,0,q_z;\omega)\\&=i\omega\,\frac{4\pi}{c^2\left[\tilde{q}^{\,2}-\kappa\left(\dfrac{\omega}{c}\right)^2\right]}\,\mathbf{j}_t(q,0,-;\omega)\\&=i\omega\,\frac{4\pi}{c^2\left[\tilde{q}^{\,2}-\kappa\left(\dfrac{\omega}{c}\right)^2\right]}\,\mathbf{j}_y(q,0,-;\omega).\end{aligned}$$

Thus the induced field points in the y direction. We can drop the vector notation:

$$E_{\rm ind}(q,0,q_z;\omega)=i\omega\,\frac{4\pi}{c^2\left[\tilde{q}^{\,2}-\kappa\left(\dfrac{\omega}{c}\right)^2\right]}\,j(q,0,-;\omega).$$

We want the z dependence of the induced field, which is obtained by taking the inverse Fourier transform of this expression with respect to q_z. The result is

$$\begin{aligned}E_{\rm ind}(q,0,z;\omega)&=i\omega\,\frac{2\pi}{c^2\sqrt{q^2-\kappa(\omega/c)^2}}\\&\quad\times j(q,0,-;\omega)e^{-\sqrt{q^2-\kappa(\omega/c)^2}|z|}\\&=i\omega\,\frac{2\pi}{c^2\sqrt{q^2-\kappa(\omega/c)^2}}\,\sigma(q,\omega)\\&\quad\times E_{\rm tot}(q,0,z=0;\omega)\\&\quad\times e^{-\sqrt{q^2-\kappa(\omega/c)^2}|z|}\\&=\frac{\left(\dfrac{\omega}{\tilde{c}q}\right)^2}{\gamma(q,\omega)}\left[\frac{i2\pi q}{\kappa\omega}\,\sigma^t(q,\omega)\right]\\&\quad\times E_{\rm tot}(q,0,z=0;\omega)\\&\quad\times e^{-\gamma(q,\omega)q|z|}.\end{aligned}$$

The expression inside the square brackets is the transverse analogue of the polarizability in two dimensions. In the plane we have

$$\begin{aligned}E_{\rm ind}(q,0,z=0;\omega)&=\frac{\left(\dfrac{\omega}{\tilde{c}q}\right)^2}{\gamma(q,\omega)}\left[\frac{i2\pi q}{\kappa\omega}\,\sigma^t(q,\omega)\right]\\&\quad\times E_{\rm tot}(q,0,z=0;\omega),\end{aligned}$$

and in the second plane

$$\begin{aligned}E_{\rm ind}(q,0,|z|=d;\omega)&=\frac{\left(\dfrac{\omega}{\tilde{c}q}\right)^2}{\gamma(q,\omega)}\left[\frac{i2\pi q}{\kappa\omega}\,\sigma^t(q,\omega)\right]\\&\quad\times e^{-\gamma(q,\omega)qd}E_{\rm tot}(q,0,z=0;\omega).\end{aligned}$$

We get the contribution to the interaction energy from this s-polarized interaction by using the same expressions as in the nonretarded interaction with the replacements:

$$\begin{aligned}\alpha_0(q;\omega)\to\tilde{\alpha}_0^t(q;\omega)&=\frac{-\left(\dfrac{\omega}{\tilde{c}q}\right)^2}{\gamma(q,\omega)}\,\alpha_0^t(q;\omega)\\&=\frac{-\left(\dfrac{\omega}{\tilde{c}q}\right)^2}{\gamma(q,\omega)}\left[\frac{i2\pi q}{\kappa\omega}\,\sigma^t(q,\omega)\right],\\c_q\to c_{q,\omega}&=e^{-\gamma(q,\omega)qd}.\end{aligned}$$

The conductivity is

$$\sigma^t(q,\omega)=i\,\frac{\rho_0e^2}{m^*\omega}+i\,\frac{\Pi(\omega)}{\hbar\omega},$$

where $\Pi(\omega)$ is the current-current correlation function. The first term dominates completely in the expression for the interaction energy. Thus we do not really need the current-current correlation for the present problem. However, it may be useful in other situations so we give it here anyhow. We find it is

$$\begin{aligned}\Pi(Q,iWQ)=-\frac{e^2k_0^2}{6m^*\pi}\Bigg\{&6W^2-2Q^2\\&-\sqrt{2}\,\frac{1}{Q}\,[\sqrt{(1-W^2-Q^2)^2+4W^2}\\&-(1+W^2-Q^2)]^{1/2}[\sqrt{(1-W^2-Q^2)^2+4W^2}\\&+2(1+W^2-Q^2)]\Bigg\},\end{aligned}$$

when expressed in our dimensionless variables from the main text. It is given on the imaginary frequency axis, which is where it is needed in calculations of the type performed

here. The result near the real axis, if needed, is obtained through an analytical continuation.

Transverse dielectric function

In three dimensions transverse and longitudinal dielectric functions have the same long-wavelength limits. It is also true in two dimensions as is demonstrated below. The transverse dielectric function enters the relation between the total and external fields in the following way:

$$E_{\rm tot}=\frac{\omega^2-(\tilde{c}q)^2}{\omega^2\varepsilon^t(q;\omega)-(\tilde{c}q)^2}\,E_{\rm ext}.$$

This leads to

$$\varepsilon^t(q;\omega)=1-i\omega\,\frac{2\pi}{c^2q\,\gamma(q,\omega)}\,\sigma^t(q;\omega)$$

$$+i\,\frac{2\pi q}{\omega\kappa\gamma(q,\omega)}\,\sigma^t(q;\omega)$$

$$=1+i\,\frac{2\pi q}{\omega\kappa}\,\gamma(q,\omega)\sigma^t(q;\omega).$$

Thus we have

$$\varepsilon^t(q;\omega)=1$$

$$+i\,\frac{2\pi q}{\omega\kappa}\,\gamma(q,\omega)\sigma^t(q;\omega)\quad\text{including retardation,}$$

$$\varepsilon^t(q;\omega)=1+i\,\frac{2\pi q}{\omega\kappa}\,\sigma^t(q;\omega)\quad\text{neglecting retardation.}$$

In the long-wavelength limit, neglecting retardation, we have

$$\varepsilon^t_{\rm 2D}(q,i\omega)\approx1+\frac{2\pi e^2\rho_0}{\kappa m^*}\,\frac{q}{\omega^2}\left(1-\frac{q^2\nu_F^2}{4\omega^2}\right),$$

$$\varepsilon^l_{\rm 2D}(q,i\omega)\approx1+\frac{2\pi e^2\rho_0}{\kappa m^*}\,\frac{q}{\omega^2}\left(1-\frac{3q^2\nu_F^2}{4\omega^2}\right),$$

where ν_F is the Fermi velocity. Including retardation we have

$$\varepsilon^t_{\rm 2D}(q,i\omega)\approx1+\frac{2\pi e^2\rho_0}{m^*\kappa}\,\frac{q}{\omega^2}\,\gamma(q,i\omega)\left(1-\frac{q^2\nu_F^2}{4\omega^2}\right),$$

$$\varepsilon^l_{\rm 2D}(q,i\omega)\approx1+\frac{2\pi e^2\rho_0}{m^*\kappa}\,\frac{q}{\omega^2}\,\gamma(q,i\omega)\left(1-\frac{3q^2\nu_F^2}{4\omega^2}\right).$$

[1] H. B. G. Casimir and D. Polder, Phys. Rev. **73**, 360 (1948); H. B. G. Casimir, J. Chim. Phys. Phys.-Chim. Biol. **47**, 407 (1949).

[2] In the original work of Casimir he treated the force between two thick metallic plates or walls and found the force was independent of the material parameters. He used totally reflecting boundary conditions. In the case of two dielectric plates where the long-wavelength fields are not totally reflected the result depends on the dielectric properties of the media. In general, the Casimir force depends on the boundary conditions and the shape of the boundaries. Some examples: if a spherical shell is split in two pieces the Casimir force between the pieces is repulsive instead of attractive; the force between a wall and a halfsphere, like in the experimental setup of Ref. 7, depends on the radius of the sphere; the force between a perfectly conducting plate and an infinitely permeable plate is repulsive (Ref. 24); the concept of Casimir force has grown with time and come to include not only the force between macroscopic objects with distinct boundaries but also, e.g., the force between an atom and a plate in which case the force depends on the properties of the atom.

[3] D. Kleppner, Phys. Today **43** (10), 9 (1990).

[4] P. W. Milonni and M.-L. Shih, Contemp. Phys. **33**, 313 (1992), and references therein.

[5] E. Elizalde and A. Romeo, Am. J. Phys. **59**, 711 (1991).

[6] V. M. Mostepanenko and N. N. Trunov, Usp. Fiz. Nauk **156**, 385 (1988) [Sov. Phys. Usp. **31**, 965 (1988)]; G. Plunien, B. Müller, and W. Greiner, Phys. Rep. **134**, 87 (1986).

[7] S. K. Lamoreaux, Phys. Rev. Lett. **78**, 5 (1997).

[8] J. Schmit and A. A. Lucas, Solid State Commun. **11**, 415 (1972).

[9] R. A. Craig, Phys. Rev. B **6**, 1134 (1972).

[10] N. G. Van Kampen, B. R. A. Nijboer, and K. Schram, Phys. Lett. **26A**, 307 (1968).

[11] E. M. Lifshitz, Zh. Eksp. Teor. Fiz. **29**, 94 (1955) [Sov. Phys. JETP **2**, 73 (1956)].

[12] T. J. Gramila, J. P. Eisenstein, A. H. MacDonald, L. N. Pfeiffer, and K. W. West, Phys. Rev. Lett. **66**, 1216 (1991).

[13] L. Wendler and R. Pechstedt, Phys. Status Solidi B **138**, 197 (1986).

[14] F. Stern, Phys. Rev. Lett. **18**, 546 (1967).

[15] D. A. Dahl and L. J. Sham, Phys. Rev. B **16**, 651 (1977).

[16] A. V. Chaplik and M. V. Krasheninnikov, Surf. Sci. **98**, 533 (1980).

[17] G. F. Giuliani and J. J. Quinn, Phys. Rev. B **26**, 4421 (1982).

[18] S. Das Sarma and A. Madhukar, Phys. Rev. B **23**, 805 (1981).

[19] T. Ando, A. B. Fowler, and F. Stern, Rev. Mod. Phys. **54**, 437 (1982).

[20] M. O. Godzaev and Bo E. Sernelius, Phys. Rev. B **33**, 8568 (1986), and references therein.

[21] T. M. Rice, Ann. Phys. **31**, 100 (1965).

[22] D. Langbein, *Van der Waals Attraction*, Springer Tracts in Modern Physics Vol. 72 (Springer-Verlag, Berlin, 1974), p. 24.

[23] F. Zhou and L. Spruch, Phys. Rev. A **52**, 297 (1995).

[24] V. Hushwater, Am. J. Phys. **65**, 381 (1997).

[25] L. Zheng and A. H. MacDonald, Phys. Rev. B **49**, 5522 (1994).

[26] L. Świerkovski, J. Szymański, and Z. W. Gortel, Phys. Rev. Lett. **74**, 3245 (1995).